EFFECT OF STRAIN HARDENING LAYER ON PITTING FORMATION UNDER ROLLING CONTACT

C. H. Chue and H. H. Chung

Department of Mechanical Engineering, National Cheng Kung UniversityTainan, Taiwan 70101

ABSTRACT

The role of the strain-hardened layer playing in pitting formation during rolling contact is analyzed using the fracture mechanics approach. The other governing factors are the initial crack length, crack angle, contact force, friction on all contact surfaces, and the hydraulic pressure of trapped fluid acting on the crack surfaces. The strain energy density factors are calculated by application of the two-dimensional finite element method. The strain energy density theory is applied to show the coupling effects between the hardened layer and the other factors. All analytical results predicted in this paper agree well with the experimental observations.

1 INTRODUCTION

The research on rolling contact problem with defects has been a long time and extensive [1-5]. **T**hree layers**,** ratchetting layer, elastic/plastic shakedown layer and elastic layer**, are** formed near the surface of substrate. In this paper, the coupling effects of strain-hardened layer with the initial crack length, crack angle, contact force, friction on all contact surfaces, and the hydraulic pressure of trapped fluid applied on the crack surfaces, on pit formation are studied. The strain energy density theory [6] is used to predict the fracture behavior of the surface crack under rolling contact.

2 PROBLEM STATEMENT

The two-dimensional model used in this analysis is illustrated in Figure 1. A rigid circular cylindrical roller runs over an elastic plate of W = 1.5 mm long and H = 0.55 mm high represents the elastic half-space. The Young's modulus E_p and the Poisson's ratio ν_p of the elastic plate are 282 GPa and 0.3, respectively. An inclined surface crack of length a makes an angle β with the surface in rolling x-direction. The rigid cylindrical roller with radius R = 2.49 mm initially indents on the plate surface with downward displacement d. The roller is assumed to have a downward displacement d such that the vertical reaction force between the roller and half surface is P = 1957 N. In this paper, d = 0.006 mm is used for P = 1957 N. After the indentation, the roller runs at a velocity V = 0.0838 mm/sec and rotates at an angular velocity ω = 0.01 radian/sec from left end position x = -0.2 mm to the right x = 0.3028 mm. The bottom of the plate is assumed fixed and the two sides are allowed to move in y-direction only. The depth h denotes the thickness of the strain-hardened layer. In the analysis, the

Poisson's ratio ν_L of the layer is assumed to be equal to ν_p while the Young's modulus E_L is subjected to change.

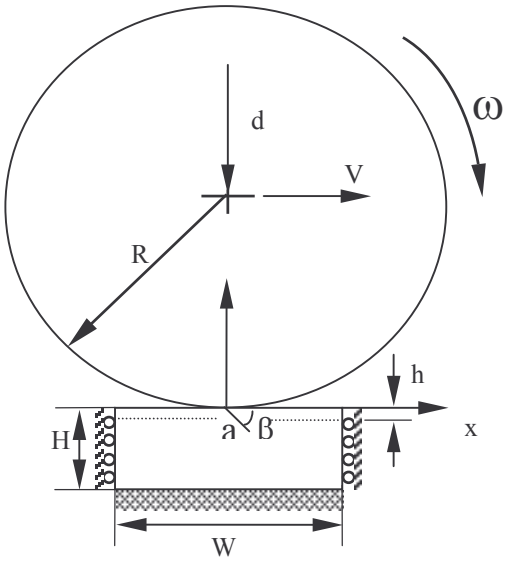

Figure 1. Schematic of rigid circular roller on cracked plate.

RESULTS AND DISCUSSIONS

3.1. Critical pressure

Before going into the discussion of the results, the term "critical pressure" used to characterize the pitting phenomena has to be defined. Figures 2 and 3 show a typical case of the occurrences of k_i and S_{min} vs. location of the rigid body center x for a = 0.012 mm, $\beta = 25^0$, d =0.006 mm , $\mu = 0.1$ and p = 1020 MPa. Consider the point A in Figure 2, where the value of k_1 is maximum and at the same time k_2 is negative. If the minimum strain energy density S_{min} is computed at that point, it will be shown in Figure 3, i.e. point A. According to strain energy density theory, as S_{min} reaches S_C, the crack will propagate along a positive angle θ_0. It means that the crack will propagate toward the horizontal direction. If the analyses are kept on going, the final crack path becomes a pit.

Now, consider the point B in Figure 2 where k_2 is maximum and positive. At this time, the crack is totally compressed and k_1 is almost zero. Its S_{min} is also shown in Figure 3. Again, as S_{min} reaches S_C, the crack will propagate downward. In some cases, k_1 increases abruptly after running over the crack mouth and reaches maximum at point C. After point C, k_1 decreases to zero. In this period, k_2 is positive. The strain energy density theory predicts that the crack would propagate downward.

If the hydraulic pressure p increases, the values of k_i and S_{min} at point A will increase. As S_{min} at point A greater than that at point B or C, the pitting will occur and the p is defined as the "critical pressure" p_{cr}.

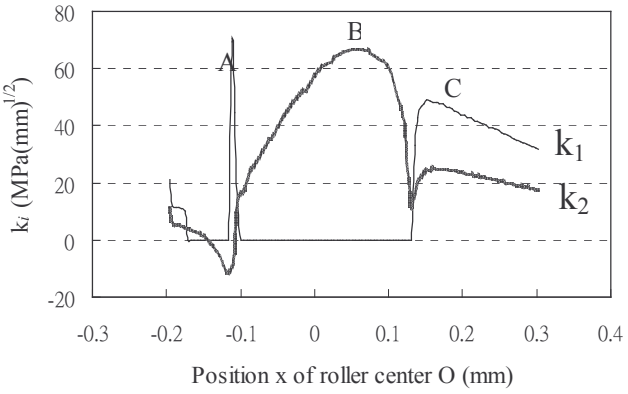

Figure 2. Variations of stress intensity factors k_1 and k_2 with roller center O (a = 0.012 mm, β =25^0,d=0.006 mm and μ = 0.1).

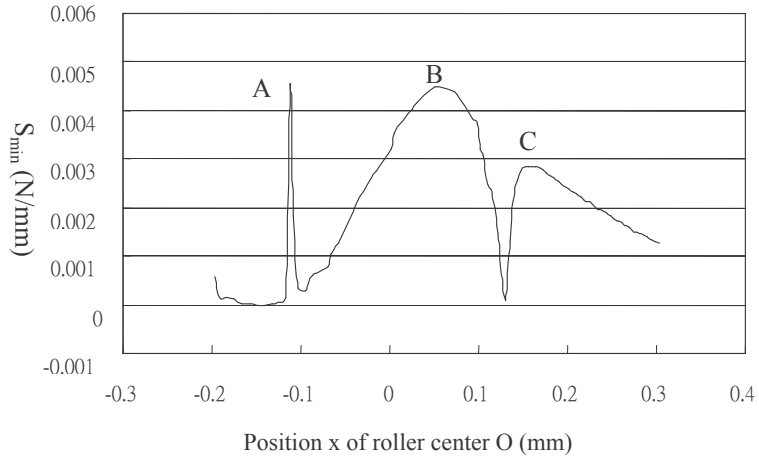

Figure 3. Variations of minimum strain energy density factor S_{min} with roller center O (a = 0.012 mm, β =25^0, d = 0.006 mm and μ = 0.1).

3.2. Indentation force

For a = 0.012 mm, β = 25^0, μ = 0.05 and h = 0.01 mm, Figure 4 shows the relation between the critical hydraulic pressure and indentation depth d when $E_L = E_p$, $1.4E_p$ and $3E_p$. For higher indentation force, it requires larger critical hydraulic pressure to open the crack. Also, as the hardened layer becomes stiffer (i.e. higher E_L), it results in smaller crack opening displacement and S_{min} at point A. For creating a pit, higher critical pressure is needed to make $(S_{min})_A$ larger than $(S_{min})_B$ or $(S_{min})_C$.

3.3. Initial crack length

The effect of initial crack length a on the formation of pitting can be determined if the hardened layer is considered. It depends on the fact that the crack tip is inside the layer or not. For β = 25^0, d = 0.006

mm, μ = 0.05 and h = 0.01 mm, Figure 5 shows the relations between the critical pressure and the initial crack length when $E_L = E_p$, $1.4E_p$ and $3E_p$. If a = 0.012 mm, higher p_{cr} is required for stiffer layer. In the cases of a = 0.06mm or larger, the crack tip is far away from the interface of hardened layer and base material. It makes no difference to consider the existence of the layer. More complicate situations are arisen when a = 0.024mm or 0.036mm.

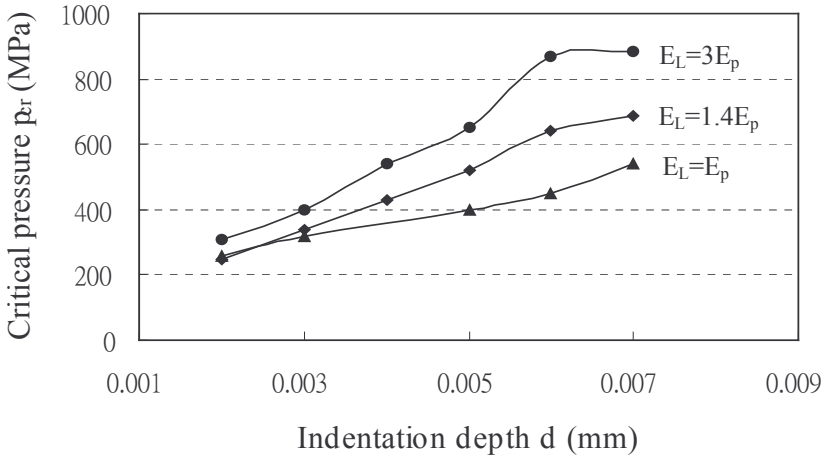

Figure 4. Variations of critical pressure p_{cr} with indentation depth d for different E_L (a = 0.012 mm, $\beta = 25^0$, μ = 0.05 and h = 0.01 mm).

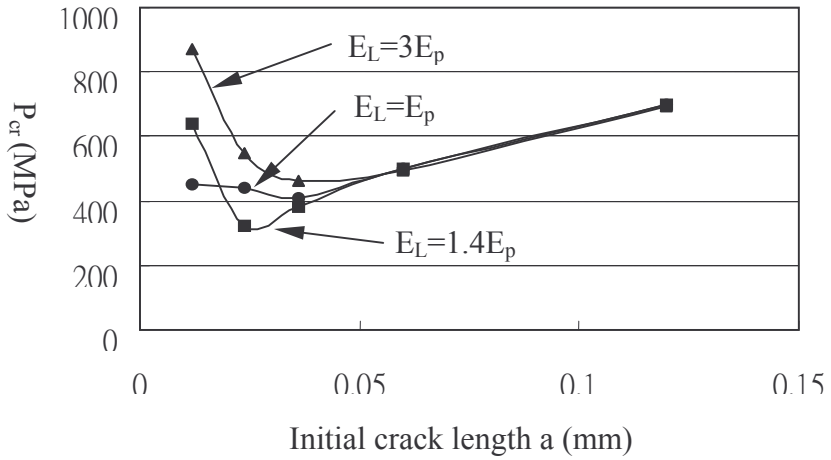

Figure 5. Critical pressure p_{cr} with crack length a at different E_L ($\beta = 25^0$, d = 0.006, μ = 0.05 and h = 0.01 mm).

3.4. Coefficient of friction

Figure 6 shows the relation between critical pressure and coefficient of friction μ at different E_L for a = 0.012 mm, $\beta = 25^0$, d = 0.006 mm and h = 0.01 mm. For dry rollers with high μ [5], pit did not form. Pit formation was rapid in good lubricant conditions where friction was low. This conclusion can be seen from Fig. 9 that higher critical pressure is required for higher coefficient of friction to form pits. As the strain hardened surface layer becomes stiffer, it requires higher hydraulic pressure to create a pit. At the condition $E_L = 3E_p$ and $\mu = 0.4$ which is not shown in the figure, $(S_{min})_A$ will never exceed $(S_{min})_B$.

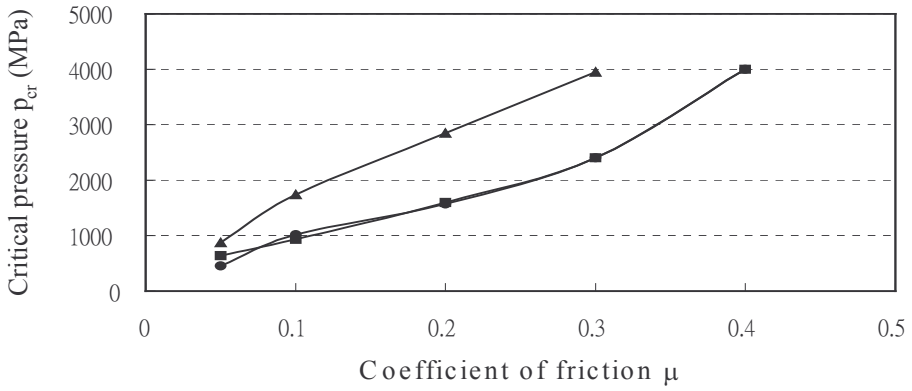

Figure 6. Critical pressure p_{cr} with μ at different E_L (a = 0.012 mm, $\beta = 25^0$, d = 0.006 mm and h = 0.01 mm).

3.5. Strain hardened surface layer thickness

Figure 12 plots the varitaion of p_{cr} with layer thickness h. It shows that the critical pressure decreases initially and then increases. For the cases with h < 0.1mm, the layer behaves as a beam rested on the elastic foundation (the base material). As the roller runs after the crack mouth, the crack opens due to bending effect. At this moment (i.e. point C), k_1 in Figure 3 reaches a maximum and $(S_{min})_C > (S_{min})_B$. Consequently, the hydraulic pressure has to be high enough such that $(S_{min})_A > (S_{min})_C$. From the finite element results, it shows that $(S_{min})_C$ decreases with increasing thickness h (h < 0.1mm). As a result, the required hydraulic pressure for creating a pit becomes small when h < 0.1mm.

As h $\geqq$ 0.1mm, most of the plate becomes stiffer. The intensity k_2 at point B in Figure 3 dominates and $(S_{min})_B > (S_{min})_C$. Consequently, the pressure acting on the crack surface should be large enough such that $(S_{min})_A > (S_{min})_B$. Thus, high critical pressure is required for h $\geqq$ 0.1mm.

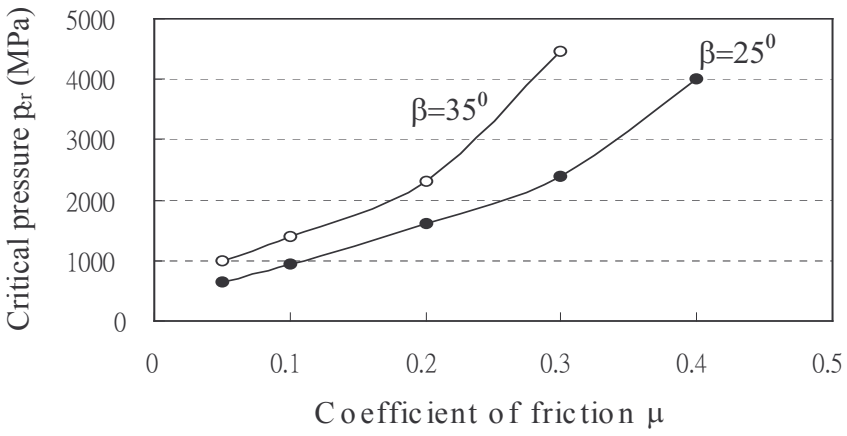

Figure 11. Variations of critical pressure p_{cr} with coefficient of friction μ for different crack angles (a = 0.012 mm, d = 0.006 mm, h = 0.01 mm and E_L=1.4E_p).

5 REFERENCES

[1] L. M. Keer, M. D. Bryant, A pitting model for rolling contact fatigue, ASME J. Lubrication Technology 105 (1983) 198-205.

[2] M. Kaneta, H. Yatsuzuka, Y. Murakami, Mechanism of crack growth in lubricated rolling/sliding contact, ASLE Trans. 28 (3) (1985) 407-414.

[3] Y. Murakami, M. Kaneta, H. Yatsuzuka, Analysis of surface crack propagation in lubricated rolling contact, ASLE Trans. 28 (2) (1985) 60-68.

[4] A. F. Bower, The influence of crack face friction and trapped fluid on surface initiated rolling contact fatigue cracks, ASME J. Tribology 110 (1988) 704-711.

[5] S. Way, Pitting due to rolling contact, ASME J. Appl. Mech. 2 (1935) A49-A58.

[6] G. C. Sih, Strain-energy-density factor applied to mixed mode crack problems, Int. J. Fract. 10 (1974) 305-321.